IOP Concise Physics

An Introduction to Plasma Physics and its Space Applications, Volume 1

Fundamentals and elementary processes

Luis Conde

Chapter 4

The ideal plasma parameters

The *ideal* plasma in thermodynamic equilibrium is introduced as a macroscopic system of interacting particles as well as the relation between the elementary processes at microscopic level with the non-equilibrium states of a plasma. These concepts are employed to introduce the characteristic time and length scales of the *ideal Maxwellian plasma*. Specifically, the Debye length, plasma frequencies and the coupling and plasma parameters. The effect of an external magnetic field and the plasma London length is discussed as well.

4.1 The ideal Maxwellian plasma

The elementary kinetic theory of thermodynamic equilibrium plasma state makes use of statistical concepts for the physical description of neutral gases introduced in chapter 3. As we have seen in section 3.2 the Maxwell–Boltzmann distribution $f_{mb}(\boldsymbol{v})$ or $g_{mb}(E)$ characterizes the equilibrium state of a single-component gas. Furthermore, the macroscopic properties of gas mixtures composed of two different interacting molecules can be described using two probability distributions with equal temperatures.

Following these basic principles we can formulate a simple model for the *thermodynamic equilibrium state* of an *ideal plasma* using the Maxwell–Boltzmann probability distribution functions as we did for multicomponent neutral gases. This concept will allow us to discuss the characteristic length and time scales of plasma phenomena such as the Debye length and plasma frequencies.

Partially ionized gases at low pressures are *ideal plasmas* where the potential energy of long-range Coulomb interaction is small compared with the average kinetic energy of the particles. In the *thermodynamic equilibrium* the macroscopic variables of these systems are uniform and do not experience temporal changes. However, a continuous activity takes place at microscopic level where ions, electrons and neutral atoms exchange energy by means of a number of collisional processes.

doi:10.1088/2053-2571/aae132ch4

To preserve the plasma state as steady and the energy of the system constant in time, the effect of each type of collisional encounter must be compensated exactly with the effect of the inverse process at atomic and molecular level. For example, the emission of light produced in collisions between electrons and neutrals is balanced with photon absorption by gas atoms, the ionizing collisions are equilibrated with ion–electron recombination processes, etc.

In its general formulation, this *principle of detailed balancing* expresses the thermodynamic reversibility at the microscopic scale. It states in essence that, under conditions of thermodynamic equilibrium, any molecular or atomic encounter is equally as likely as its reverse collisional process[1]. A direct connection exists between the plasma equilibrium state and the nature and characteristics of elementary processes at atomic and molecular scale. Specifically, we can establish the following.

A plasma or any isolated physical system composed of a large number of interacting particles is in *complete thermodynamic equilibrium* (CTE) when collisions and photo-processes are balanced by their reverse reactions.

The next step is to analyze the specific physical properties that a system of electrons, neutral atoms and positively charged particles must satisfy in the macroscopic equilibrium state,

1. The mean number densities of electrons n_e, ions n_i and neutral atoms n_a are uniform and constant over time. The thermal motion of particles only produces small local fluctuations in the densities δn_i, δn_e and δn_a of plasma species.
2. As in neutral gases, there is no average motion of plasma particles and therefore no transport of charge[2] (electric current), mass, energy or momentum.
3. The plasma is said to be *quasineutral* in the equilibrium state of electric charge. The average negative ($\rho_e = -en_e$) and positive ($\rho_i = +en_i$) electric charge densities are equal $n_i \simeq n_e = n_o$ to preserve the macroscopic charge neutrality. Therefore,

$$\nabla \cdot \boldsymbol{E} = \frac{e}{\varepsilon_o}(n_i - n_e) \simeq 0 \tag{4.1}$$

   the electric field $\boldsymbol{E} \simeq 0$ is negligible and the uniform spatial profile of the electric potential $\phi(\boldsymbol{r}) \simeq \phi_o$, is also denominated *plasma potential*.
4. The small fluctuations of the electric field $\delta \boldsymbol{E}$ are related to the variations of charged particle densities δn_e and δn_i produced by the random motion of

[1] This principle also applies to transitions (vibrational, rotational, etc) between molecular and atomic energy levels produced by collisions. For simplicity, in the following we will mainly concentrate on translational degrees of freedom and devote less attention to the chemical nature and structure of gas molecules.

[2] Furthermore, the plasma self-magnetic field is null because no electric current flows through the plasma.

charged particles. Additionally, $(\delta n_e/n_e) \ll 1$ so that, the densities of charged particles $n_e \simeq n_i = n_o$ are large enough to shield the small perturbations of the electric field.

5. The energy of the isolated quasineutral plasma is preserved. In the state of thermodynamic equilibrium[3] the average macroscopic energy density and temperature are uniform and constant in time.

The energy transfer between CTE plasma species is optimal in thermal equilibrium. All collision frequencies (2.4) are large enough to rapidly re-distribute the energy fluctuations[4] to hold the macroscopic energy density uniform and constant over time.

Under the above conditions of strict thermodynamic equilibrium the electron, ion and neutral atom populations ($\alpha = e, i, a$) can be characterized by the probability distribution function (3.5) or (3.7),

$$f_\alpha(\boldsymbol{v}) = \left(\frac{m_\alpha}{2\pi k_B T}\right)^{3/2} \exp\left(-\frac{m_\alpha\, v_\alpha^2}{2k_B\, T}\right)$$

and plasma species are in *thermal equilibrium* in this *ideal Maxwellian* CTE *plasma*. It can be physically characterized by its thermodynamic magnitudes; the equilibrium pressure, volume and temperature. The velocity distributions of plasma species are Maxwellians having average kinetic energy e_α higher than the potential energy of Coulomb interaction. Furthermore, the emitted electromagnetic radiation corresponds to black-body spectrum described by Planck's law.

Using equation (3.11) the average kinetic energy per particle $\langle\, m_\alpha v_\alpha^2/2 \,\rangle$ of each plasma specie only depends on the temperature,

$$e_\alpha = \frac{3}{2}\, k_B\, T \tag{4.2}$$

The *cold plasma* limit $T \simeq 0$ corresponds to a *monoenergetic* population where all particles have the same velocity and equations (3.5) or (3.7) can be approximated by a Dirac delta function. In *finite temperature* plasmas where $k_B T > 0$ particles have an average *thermal energy* e_α and the particle velocities are distributed around an average speed. However, the ion and electron mean thermal speeds $\bar{v}_i = \langle\, v_i \,\rangle$ and $\bar{v}_e = \langle\, v_e \,\rangle$ from equation (3.13) are different,

$$\bar{v}_e = \sqrt{\frac{8\, k_B\, T}{\pi\, m_e}} \quad \text{and,} \quad \bar{v}_i = \sqrt{\frac{8\, k_B T}{\pi\, m_i}} = \bar{v}_e \sqrt{\frac{m_e}{m_i}}$$

because of the disparity between ion and electron masses.

[3] This restrictive requisite implies that electromagnetic radiation resulting from photoprocesses cannot escape from the plasma and are absorbed back. Strictly speaking, CTE plasmas are *optically thick* and only emit blackbody radiation following Planck's law.

[4] Equivalently, the eventual deviations from the Maxwell–Boltzmann energy distribution function relax back to this equilibrium distribution much faster than any other time scale of the system.

4.2 Elementary processes and steady equilibrium states

The above requirements for CTE plasmas are very restrictive and seldom achieved in practice since most systems deviate from the strict thermodynamic equilibrium. When plasmas are limited to a physical length scale L_s the *principle of detailed balancing* is only partially accomplished. The elementary processes can have different cross sections introducing dissimilar length λ_c and time $\tau_c = 1/\nu_c$ scales for the forward and backward collisional processes. For example, the imbalance photon capture and emission processes allow the electromagnetic radiation to escape from the plasma region, the ionization and recombination rates are not equal, etc

Relaxing the rigorous conditions for the thermodynamic equilibrium we can introduce a *hierarchy* of *non-equilibrium states* for plasmas that reflect the disparity of time and length scales of elementary processes at the microscopic level.

> The plasma is in *local thermal equilibrium* (LTE) when all collisional processes are balanced (ionization, recombination, etc) but not the photoprocesses.

The LTE plasmas[5]—also called *thermal plasmas*—are collision-dominated and the electromagnetic absorption and/or emission processes can be neglected in this equilibrium. In these conditions, the electromagnetic radiation can leave the plasma[6], the macroscopic energy of the system is not conserved, therefore LTE plasmas are sustained by an external source of energy.

The LTE approximation has the implicit assumption of the existence of fast energy relaxation processes, or equivalently, of high collision frequencies (2.4). Energy fluctuations relax fast to a *local equilibrium state* on time and length scales much shorter than those of macroscopic plasma properties. The collisional energy transfer between plasma species is optimal, leading to equal temperatures of electrons ions and neutral atoms. Consequently, LTE plasmas can be characterized *locally* and the translational speeds of particles ($\alpha = e, i, a$) can be described by a *local* Maxwellian velocity distribution function with a common temperature,

$$f_\alpha(\boldsymbol{v}, \boldsymbol{r}, t) = \left(\frac{m_\alpha}{2\pi k_B T(\boldsymbol{r}, t)}\right)^{3/2} \exp\left(-\frac{m_\alpha\, v_\alpha^2}{2k_B\, T(\boldsymbol{r}, t)}\right) \tag{4.3}$$

The LTE plasmas can be considered as electrically conducting fluids in which the particle densities $n_\alpha(\boldsymbol{r}, t)$ are in *local* thermal equilibrium at the temperature $T_\alpha(\boldsymbol{r}, t)$. Their macroscopic properties are evaluated as averages of equation (4.3) over length $L_s \gg \lambda_c$ and time $\tau_s \gg 1/\nu_c$ scales much greater than those involved on microscopic particle encounters.

---

[5] This concept receives different names in the literature. It is denominated by some authors [1] *local thermodynamic equilibrium* because strictly speaking, it is not a state of *global* thermodynamic equilibrium.

[6] This is commonly used in astrophysics when the mean free path of photons is long compared with the length scale over which the temperature is changing, as in the atmosphere of stars.

We can consider next the more frequent situation in which only *some collisional processes are balanced* by the reverse encounters at the molecular level, as follows.

> The plasma is in *partial local equilibrium* (PLE) when only a small number of elementary processes are balanced.

This is the most probable situation when the plasma is confined to a limited volume, as in the laboratory and in many other physical systems. For example, for the neutral atom A the production of ions by electron impact $A + e^- \rightleftharpoons 2e^- + A^+$ is more likely than the reverse recombination process involving a three-particle collision. In low pressure PLE plasmas the ions are usually produced within the plasma bulk but leave the experimentation volume and are captured by the walls of the plasma container without experiencing a recombining collision.

In PLE plasmas the energy coupling between particles is much weaker than in LTE plasmas because the collision frequencies (2.4) are lower and the average kinetic energy per particle of ions and electrons can be different. The collisions cannot redistribute energy between plasma species and the average kinetic energy of ions, electrons and neutral atoms can be different. The available energy is not equally shared by all degrees of freedom of the system and in this *non-equilibrium* plasma the equipartition theorem discussed in section 3.6 is not accomplished.

This lack of thermal equilibrium introduces the coexistence of particle populations with different kinetic temperatures. PLE plasmas are usually found in a *multithermal equilibrium* state where each charged specie is characterized by a velocity distribution function different from equation (3.5) or (3.7) and/or can be approximated by Maxwellians with different kinetic temperatures[7].

4.3 Energy thermalization

In ideal plasmas the processes of energy exchange between the different particle species are determined by the nature and frequency of collisions at the microscopic level. The *energy thermalization* is the process by which a system of many interacting particles reaches the thermodynamic equilibrium state where available energy is equally shared (see section 3.6) amongst all energetically accessible degrees of freedom of a system.

In partially ionized plasmas where $n_a \gg (n_i, n_e)$ the short-range elastic encounters of ions and electrons with neutral atoms are the dominant processes. The *collisional energy thermalization* can be understood with the help of the calculations of box 4.1 where we calculate the energy transfer δ_E in one electron–atom and ion–atom elastic encounters.

[7] This concept can be generalized to the internal degrees of freedom of molecules and *vibrational* and *rotational* temperatures are also defined in addition to the above *translational* T_e and T_i temperatures.

Box 4.1. Electron–atom collisional energy exchange

Setting in equation (2.1) $\cos^2\theta_b \simeq 1$ we can estimate the maximum collisional energy transfer between electrons, ions and neutrals in short-range elastic collisions. The ion and neutral atom have approximately the same mass and thus $m_i \simeq m_a$ and we have,

$$\delta_E = \frac{E_i}{E_a} = \frac{4\, m_i\, m_a}{(m_a + m_i)^2} \simeq 1$$

The mass of a proton (or neutron) is $m_p = 1840 \times m_e$ the electron mass m_e and for the neutral atom $m_a = Z \times 1840 \times m_e$ where Z is the atomic mass number (nucleon number) we have,

$$\delta_E = \frac{E_a}{E_e} = \frac{4\, m_e\, m_a}{(m_a + m_e)^2} \simeq 2.2 \times 10^{-3}/Z$$

This low δ_E express the small amount of energy transfer between the electron and the neutral atom in one elastic collision. A number of encounters $N_c \times \delta_E = E_a/E_e \sim 1$ are needed to equal the energy of electron and neutral atoms. This gives $N_c \sim 1800$ for helium ($Z = 4$), $N_c \sim 18\,000$ in argon ($Z = 40$) and $N_c \sim 59\,000$ for xenon ($Z = 131$).

The energy coupling is very efficient between ions and neutral atoms $\delta_E = E_i/E_a \simeq 1$, whereas we have $\delta_E = E_a/E_e \sim 10^{-4}$ or lower for electron–atom encounters due to their dissimilar masses. The lighter electron moves faster and requires a number N_c of elastic collisions per electron to transfer its kinetic energy $N_c \times \delta_E = E_a/E_e \sim 1$ to neutral atoms. Conversely, ions and atoms reach fast equal average kinetic energy per particle.

In the steady state, the number of elastic encounters per unit of time is determined by the collision frequencies ν_{ea} and ν_{ia} that are proportional to the neutral gas pressure $n_a \sim p_a$ (equation (2.4)). In partially ionized plasmas, the thermal equilibrium (LTE) of electrons ions and gas atoms requires large collision frequencies, or equivalently, high gas pressures. Non-thermal (PLE) equilibrium occurs at lower pressures where energy coupling between plasma particles is weaker.

This effect of collisional energy coupling in the LTE–PLE transition is illustrated in figure 4.1 where are represented the argon gas T_a and electron T_e temperatures as a function of the pressure. LTE plasmas require a fast collisional energy transfer between plasma species to reach the thermal equilibrium described by the Maxwellian velocity distribution (4.3). The collision-dominated *thermal plasma* where $T_e = T_a$ and $T_a = T_i$ corresponds to high gas pressures at the right of the solid vertical line where the energy coupling between ions and neutral atoms is very efficient.

The collisional energy transfer between electrons and ions is slower at low gas pressures and the average kinetic energy of atoms and electrons becomes dissimilar.

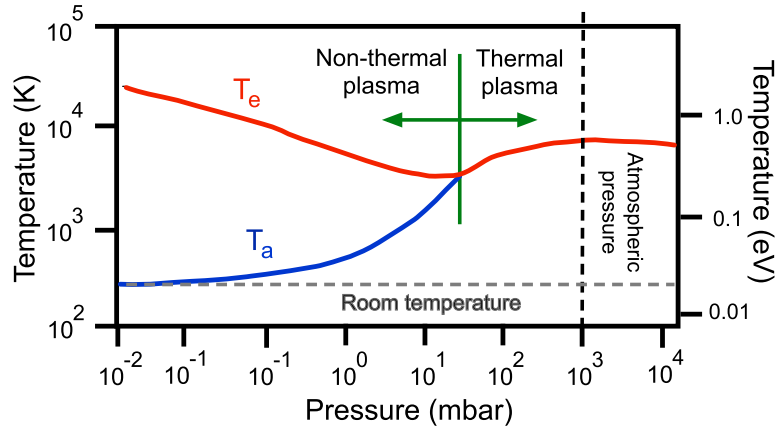

Figure 4.1. The representation of the electron T_e and neutral argon T_a temperatures as a function of the pressure p_a shows the transition from *thermal* (LTE) to *non-thermal* (PLE) partially ionized plasmas. From reference [2].

The electron temperature T_e is higher than the gas temperature $T_a \simeq T_i$ for gas pressures below $p_a = 10$ mbar at the left of the solid vertical line in figure 4.1. Each plasma specie has its own velocity distribution function that can be different from the Maxwellian distributions (3.5) or (3.7). These *non-thermal plasmas* have different average kinetic energies for each particle species because of the slower energy transfer at low collision frequencies. The equipartition principle of section 3.6 is not accomplished in this non-equilibrium plasma.

The above discussion focuses on elastic encounters (see box 4.1) but it is important to underline the energy coupling of plasma particles in figure 4.1 is not restricted to this specific electron–atom encounter. The LTE–PLE plasma transition of figure 4.1 is driven by the energy exchange produced by a variety of collisional processes. Short-range electron collisions with atoms and ions can also produce transitions between energy levels of bounded electrons of atoms and vibrational and/or rotational energy levels of molecules and ions. The external electron can be exchanged in collisions between ions and neutral atoms, and such *charge exchange* encounters decreases the average energy of ions, etc. In chapter 6 we introduce the more relevant atomic and molecular collisions in plasmas.

Moreover, figure 4.1 is specifically concerned with *partially ionized plasmas* governed by short-range collisions with neutral atoms. When the plasma ionization degree is high or in *fully ionized plasmas* long-range Coulomb collisions are the essential mechanism for energy exchange between electrons and ions and the thermal equilibrium between plasma species requires shorter characteristic times and collisions with neutrals play a minor role.

This regime dominated by Coulomb collisions occurs when the collision frequencies between charged species $\nu_{ei}\ \nu_{ee}\ \nu_{ii} > \nu_{ea}\ \nu_{ia}$ are higher than those of encounters with neutrals. This situation requires degrees of ionization above $\alpha_g = 0.01\%$ that can be reached in some laboratory plasmas.

4.4 Electric field shielding

We will examine in more detail the *ideal Maxwellian plasma* concept previously introduced in section 4.1. We consider a quasineutral plasma of density n_o with electron and ion temperatures T_e and T_i, respectively, such as those in figure 4.1 for gas pressures below 10 mbar in stationary equilibrium.

When a constant one-dimensional electric $\boldsymbol{E}_{ex}(x)$ field is *externally applied* to the system, the initial state with uniform plasma electric potential profile breaks. Electric charges move to cancel this external perturbation; electrons are attracted towards the high potential side, whereas the ions move in the opposite direction. The energy of each charged particle in the new steady equilibrium is,

$$E_{i,\,e} = \frac{m_\alpha v^2}{2} \pm e\,\phi(x)$$

where $\phi(x)$ is the new plasma potential profile introduced by the disturbance. Due to the polarization of plasma charges, the *self-consistent* electric field *inside the plasma* $\boldsymbol{E}(x) = -\nabla\phi$ acting on each charge $\pm e$ differs from $\boldsymbol{E}_{ex}(x)$. This external electric field displaces ions and electrons that in turn produce an electric field $\boldsymbol{E}(x)$ in the plasma to cancel the external disturbance. In these conditions the Maxwellian velocity distribution (equation (3.5)) for electrons and ions becomes,

$$f_{i,\,e}(\boldsymbol{v}) = \left(\frac{m_\alpha}{2\pi k_B T}\right)^{1/2} \exp\left(-\frac{m_\alpha\, v^2 \pm 2\, e\, \phi(\boldsymbol{r})}{2k_B T}\right) \tag{4.4}$$

Integrating over the velocity $\boldsymbol{v}$ as in section 3.5 we obtain the plasma density profile for ions,

$$n_i(x) = n_o \exp\left(-\frac{e\,\phi(x)}{k_B T_i}\right) \tag{4.5}$$

and electrons,

$$n_e(x) = n_o \exp\left(\frac{e\,\phi(x)}{k_B T_e}\right) \tag{4.6}$$

The perturbed plasma is not quasineutral now because the *external* electric field $\boldsymbol{E}_{ex}(x)$ produces a one-dimensional spatial profile of electron $n_e(x)$ and ion $n_i(x)$ densities. The plasma potential $\phi(x)$ can be calculated from equations (4.5) and (4.6) using the Maxwell equation (2.6a) with appropriate boundary conditions,

$$\frac{d^2\phi}{dx^2} = -\frac{e}{\varepsilon_o}\,(n_i(x) - n_e(x)) \text{ and then,}$$

$$\frac{d^2\phi}{dx^2} = \frac{en_o}{\varepsilon_o}\,[e^{e\phi/k_B T_e} - e^{-e\phi/k_B T_i}]$$

Nevertheless, it is difficult to find analytical solutions of this nonlinear differential equation and we will not do so here. However, when the strength of the external

electric field $\boldsymbol{E}_{ex}$ is not intense the charge separation is not strong and we can assume a uniform small electric field $E(x) \simeq -E_o$ in the plasma. This gives the approximate linear plasma potential profile,

$$\phi(x) \simeq \phi_o - E_o x + O(x)^2 \text{ and we can set } \phi_o = \phi(0) = 0 \tag{4.7}$$

We make use of this approximation to illustrate the polarization of plasma charged particles in figure 4.2. The dotted line represents the linear and symmetric plasma potential profile of $\Delta\phi = \pm 0.8$ V (right axis) as a function of the x coordinate.

The normalized densities of charged particles $n_{e,i}(x)/n_o$ refer to the left axis and are given by the equations (4.5) and (4.6). Ions (solid red curves) are attracted towards negative potentials ($x < 0$), whereas electrons (solid blue curves) move to the positive plasma potential side ($x > 0$). Finally, we have $\phi(0) = 0$ and equal particle densities $n_o = n_i = n_e$ at the origin.

In figure 4.2 the local charge densities (4.6) and (4.5) depend on the ratio $|e\phi(x)|/k_B T_{i,\,e}$ between electrostatic ($e_{el} = \pm e\phi$) and thermal ($e_{th} \sim k_B T_\alpha$ in equation (4.2)) energies per particle. The dimensionless *coupling parameter* is defined for both charged ($\alpha = e,\, i$) species,

$$\Gamma_{c\alpha} = \frac{|e\phi(x)|}{k_B T_\alpha} > 0 \tag{4.8}$$

which will be examined in more detail later in section 4.5.3. In *ideal plasmas* $\Gamma_{c\alpha} < 1$ and these are said to be *weakly coupled*, whereas *coupled plasmas* with $\Gamma_{c\alpha} > 1$ are colder. In figure 4.2 for the lower electron and ion temperatures $T_e = 0.5$ eV and $T_i = 0.025$ eV we have $|e\phi(x)|/k_B T_{i,\,e} < 1$ and electrostatic energy dominates along $\Delta x = \pm 1$, whereas for all other curves thermal energy is higher and $|e\phi(x)|/k_B T_{i,\,e} > 1$.

Charged particles have low thermal energy in *non-ideal plasmas* ($|e\phi(x)|/k_B T_{i,\,e} > 1$) and their motions are essentially governed by the plasma electric

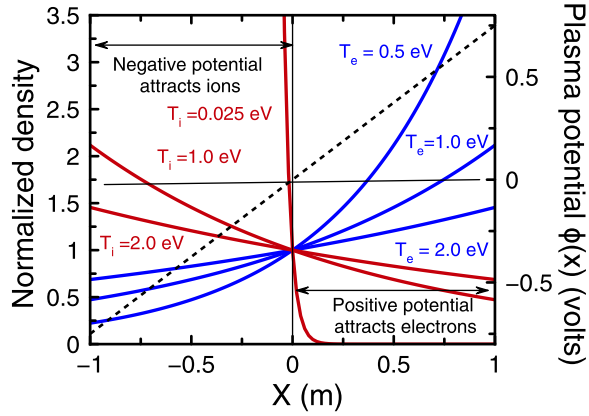

Figure 4.2. The scaled ion and electron densities $n_{i,e}(x)/n_o$ (equations (4.6) and (4.5)) for the symmetric linear plasma potential profile $\phi(x)$ (dotted line) of equation (4.7) are plotted against the coordinate x. The ion densities for $T_i = 0.025$, 1.0 and 2.0 eV are represented by a solid red line, and blue curves are the electron densities for $T_e = 0.5$, 1.0 and 2.0 eV.

field. Both species thus separate in space in figure 4.2, where low temperature ions ($T_i = 0.025$ eV) concentrate their spatial distribution $n_i(x)$ around the small range $\Delta x \sim \pm 0.25$ around the origin. The density $n_e(x)$ of cold electrons ($T_e = 0.5$ eV) decreases rapidly for $x < 0$ and is essentially localized in the electron-attracting zone where $\phi(x) > 0$.

Because of the low electron temperature, only a small fraction in the tail of the velocity distribution function (4.4) have energy enough to penetrate into the electron-repelling region ($\phi(x) < 0$, $x < 0$). In *non-ideal plasmas* where $(|e\phi(x)|/k_B T_{i,\,e}) > 1$ the stationary spatial distribution of charged particles along the plasma potential profile is concentrated by the small number of energetic charged particles in the (cold) Maxwellian distribution function having thermal energy to overcome the potential barrier.

In the opposite limit of *ideal plasma* where $|e\phi(x)|/k_B T_{i,\,e} < 1$ the particle density profiles $n_e(x)$ and $n_i(x)$ are smoother along the x axis as in the figure 4.2 for high ion and electron temperatures. The charged particles can move randomly along the plasma potential spatial profile due to their larger average kinetic energy. The increase of $n_e(x)$ along the electron repelling side $\phi(x) < 0$ (equivalently, $n_i(x)$ for $\phi(x) > 0$) with the increasing electron temperature (T_i for ions) is because the Maxwellian energy distribution $f_e(\boldsymbol{v})$ (for ions $f_i(\boldsymbol{v})$) in equation (4.4) becomes broader when T_e (T_i) grows.

Ideal plasmas have a large number of charged particles in the high energy tail of the Maxwellian distribution with energy enough to overcome the electric potential barrier, and consequently, these charged particles can move along the x axis of figure 4.2.

The preceding discussion illustrates an important property of plasmas; their *ability to shield electric fields* of moderate strength externally applied to the medium. The linear plasma potential profile (equation (4.7)) is symmetric with respect to the $x = 0$ coordinate as well as the electron and ion distributions $n_{e,i}(x)$ for the same temperature of equations (4.5) and (4.6). In *ideal* LTE *plasmas* where $T_e = T_i$, as in the figure 4.1 for gas pressures over 10 mbar, both charged species equally contribute to the shielding of the stationary disturbance introduced by the external electric field.

This is not the case for *ideal* PLE *plasmas* where electron and ion temperatures $T_e \gg T_i \simeq T_a$ are different. The steep distribution $n_i(x)$ of cold ions ($e\,\phi(x) / k_B\,T_i > 1$) at room temperature ($T_i \simeq T_a = 0.025$ eV) which is distributed around the origin due to its low thermal energy has been intentionally drawn in figure 4.2. These ions have $\Gamma_{ci} > 1$ and are *strongly coupled*, whereas the electrons that satisfy the ideal plasma condition $\Gamma_{ce} < 1$ in figure 4.2 and for $T_e > 0.5$ eV can easily penetrate the region $\phi(x) < 0$ where the ions are concentrated. The shielding of the external disturbance in this *two-temperature ideal plasma*—as for low gas pressure plasmas in figure 4.1—is essentially due to the more mobile electrons.

4.5 The plasma parameters

In addition to the collisional parameters for long- and short-range collisions between charged particles and gas atoms, additional time and length scales are needed to characterize the electromagnetic interaction between ions and electrons.

We introduce in this section the *Debye length* and the *plasma frequency* that are related to the attenuation of small amplitude spatial and temporal disturbances from the equilibrium state of a quasineutral plasma. Additionally, we will discuss more precisely the *coupling* and *plasma parameters* outlined in the previous section as well as the effects introduced by external magnetic fields.

Figure 4.3 shows the scheme of a random deviation from the plasma quasineutrality in one dimension along the distance δx, where electrons (blue dots) accumulate at one side and leave behind a density of ions (red dots). The perturbed ion densities are $\delta n_i = \delta n_e = \delta n_o$ because no additional particles are created. Outside the distance δx the plasma remains quasineutral $n_e \simeq n_i = n_o$ and is represented by equal number of blue and red dots.

Within δx an intense and localized electric field $E(x)$ is created by the charge density $\rho_c(x)$ which also can be seen as two parallel sheets of electric charge with opposite signs separated δx, their surface charge density is $\sigma_c \simeq \pm e\, \delta n_o \times \delta x$, similarly to a parallel plane capacitor.

We have seen in the previous section 4.4 that, in the absence of other forces, the charged particles driven by $E(x)$ will move to cancel the perturbation and to restore the plasma quasineutrality. The time scale τ_{pe} of charge fluctuations as in the scheme of figure 4.3 defines the *electron plasma frequency* $f_{pe} = 1 / \tau_{pe}$ and corresponds to the minimum time of response of faster plasma charges (electrons) to attenuate time dependent fluctuations.

In addition, the extension of the perturbation introduced by $E(x)$ is limited to a region δx characterized by distance λ_D denominated as *Debye length*. This distance could be also understood as the length scale along which is canceled the spatial average of electric charge in the plasma. Only the distances $L_s > \lambda_D$ over the Debye

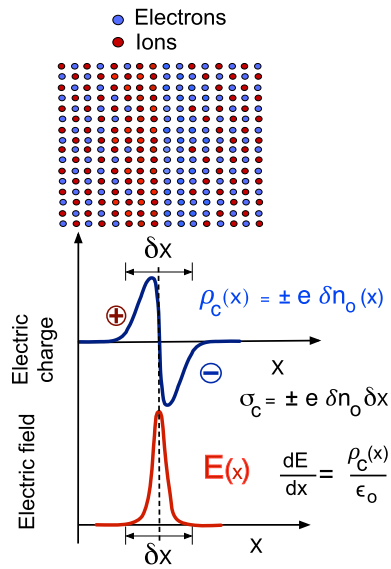

Figure 4.3. Scheme of a one-dimensional density fluctuation δn_o in a quasineutral plasma.

length are usually considered in plasma physics because for longitudes $L_s < \lambda_D$ below the electric fields are local, very variable and they are regarded as microscopic.

Finally, the electric charge shielding process discussed in section 4.4 requires a number of free charges to cancel the local electric field fluctuations of a given magnitude. This basic idea introduces the dimensionless *plasma parameter* that is closely related with the *coupling parameter* $\Gamma_{c\alpha}$ previously introduced in equation (4.8).

4.5.1 The Debye length

We again consider a quasineutral plasma ($n_e = n_i = n_o$) where a small external disturbance is introduced by the electric test charge $\delta\rho_{ext} = q\ \delta(\boldsymbol{r})$ where $\delta(\boldsymbol{r})$ is the Dirac delta function. As discussed in section 4.4, a cloud of electric charge of density,

$$\delta\rho_{sc} = e\ [n_i(\boldsymbol{r}) - n_e(\boldsymbol{r})]$$

develops in the plasma to cancel this time-independent perturbation. For the total charge density $\delta\rho$ in the plasma we can write,

$$\delta\rho = \delta\rho_{ext} + \delta\rho_{sc} = q\ \delta(\boldsymbol{r}) + e\ [n_i(\boldsymbol{r}) - n_e(\boldsymbol{r})] \tag{4.9}$$

The otherwise uniform space plasma potential profile is affected by the small local departure ($\delta\rho \neq 0$) from the electric charge balance. In the following, we will left open the possibility of having different temperatures[8] for electrons T_e and ions T_i. Aditionally, the potential energy disturbance $e\phi(\boldsymbol{r})$ is assumed small compared to the thermal energies of charged particles ($\alpha = e,\ i$),

$$\Gamma_{c\alpha} = \frac{q\ \phi(\boldsymbol{r})}{k_B\ T_\alpha} \ll 1 \tag{4.10}$$

Therefore, the *ideal plasma* approximation is satisfied or, equivalently, the plasma is *weakly coupled*. In these conditions we can approximate equations (4.5) and (4.6) by,

$$n_\alpha(\boldsymbol{r}) \simeq n_o\left(1 \pm (\frac{e\ \phi(\boldsymbol{r})}{k_B T_\alpha}) + O(\frac{e\ \phi(\boldsymbol{r})}{k_B T_\alpha})^2\right) \tag{4.11}$$

and substituting into the equation (2.6a) for the plasma potential $\phi(\boldsymbol{r})$ we have,

$$\nabla^2\phi = -\frac{\delta\rho}{\varepsilon_o} = -\frac{1}{\varepsilon_o}\left[\delta\rho_{ext} + \frac{e^2\ n_o}{k_B T_i}\ \phi(\boldsymbol{r}) + \frac{e^2\ n_o}{k_B T_e}\ \phi(\boldsymbol{r})\right]$$

We obtain a differential equation for the departure $\phi(\boldsymbol{r})$ from the equilibrium ($\phi_o \simeq 0$) of the plasma potential profile,

[8] This derivation considers two-temperature PLE plasmas and in the limit when $T_i = T_e$ is recovered the LTE thermal equilibrium.

$$\left(\nabla^2 - \frac{1}{\Lambda_D^2}\right)\phi(\boldsymbol{r}) = -\frac{q}{\varepsilon_o}\,\delta(\boldsymbol{r}) \tag{4.12}$$

The characteristic length Λ_D is,

$$\frac{1}{\Lambda_D^2} = \frac{1}{\lambda_{Di}^2} + \frac{1}{\lambda_{De}^2}$$

and λ_{Di} and λ_{De}, respectively, are the *ion* and *electron Debye lengths*,

$$\lambda_{Di} = \sqrt{\frac{\varepsilon_o\, k_B T_i}{e^2\, n_o}};\quad \lambda_{De} = \sqrt{\frac{\varepsilon_o\, k_B T_e}{e^2\, n_o}} \tag{4.13}$$

and practical expressions for the estimation of λ_D are derived in box 4.2.

Box 4.2. Calculation of the Debye lengths

The equations (4.13) are,

$$\lambda_D = \left(\frac{\varepsilon_o\, k_B\, T}{e^2\, n_o}\right)^{1/2}$$

and therefore

$$\lambda_D^2\ [\mathrm{m}] = \frac{(8.85 \times 10^{-12}) \times (1.38 \times 10^{-23})}{(1.6 \times 10^{-19})^2} \times \frac{T\ [\mathrm{K}]}{n_o\ [\mathrm{m}^{-3}]}$$
$$= 4762 \times \frac{T\ [\mathrm{K}]}{n_o\ [\mathrm{m}^{-3}]}$$

using the relation (1.1) $T[\mathrm{K}] = 11\,600 \times T\,[\mathrm{eV}]$ we have,

$$\lambda_D\ [\mathrm{m}] = 69 \times \sqrt{11\,600} \times \sqrt{\frac{T\ [\mathrm{K}]}{n_o\ [\mathrm{m}^{-3}]}} = 7433 \times \sqrt{\frac{T\ [\mathrm{eV}]}{n_o\ [\mathrm{m}^{-3}]}}$$

The plasma density $n_o[\mathrm{m}^{-3}] = 10^6 \times n_o[\mathrm{cm}^{-3}]$ is frequently expressed in cubic centimeters and we obtain a practical expression,

$$\lambda_D\ [\mathrm{m}] = 7433 \times \frac{1}{10^3} \times \sqrt{\frac{T\ [\mathrm{eV}]}{n_o\ [\mathrm{cm}^{-3}]}} = 7.43 \times \sqrt{\frac{T\ [\mathrm{eV}]}{n_o\ [\mathrm{cm}^{-3}]}}$$

and finally we obtain,

$$\lambda_D\ [\mathrm{cm}] = 743 \times \sqrt{\frac{T\ [\mathrm{eV}]}{n_o\ [\mathrm{cm}^{-3}]}}$$

and values of the Debye length λ_D for different plasmas are calculated in table 4.1.

Table 4.1. The plasma parameters for densities n_o and temperatures T of figure 1.2. The Debye length and plasma frequency are calculated as in boxes 4.2 and 4.3. The asterisk marks the *non-ideal* coupled plasmas where $\Gamma_c > 1$ in equations (4.16) and (4.17). The London lengths $\lambda_L = c/\omega_{pe}$ in equations (4.19) and (4.20) are in meters.

Plasma	n_o (cm^{-3})	T (eV)	λ_D (cm)	f_{pe} (Hz)	λ_L (m)	N_D	Γ_c	
Fusion reactor	10^{15}	10^4	2.34×10^{-3}	2.84×10^{11}	1.06×10^{-3}	336	1.65×10^{-3}	
Laser plasmas	10^{20}	100	7.40×10^{-7}	8.97×10^{13}	3.34×10^{-6}	3.36×10^{-3}	3.55	(*)
Plasma focus	10^{20}	10^3	2.34×10^{-6}	8.97×10^{13}	3.34×10^{-6}	3.36×10^{-3}	3.55	(*)
Low pressure discharge	10^{12}	2	1.05×10^{-3}	8.97×10^9	3.34×10^{-2}	3.36×10^5	1.65×10^{-5}	
Discharge tubes	10^8	2	1.05×10^{-1}	8.97×10^7	3.34	3.36×10^9	3.55×10^{-8}	
High pressure arcs	10^{17}	1	2.34×10^{-6}	2.84×10^{12}	1.06×10^{-4}	3.36	3.55×10^{-2}	
Earth ionosphere	2.5×10^5	0.05	0.33	4.49×10^6	66.9	1.34×10^{12}	6.54×10^{-10}	
Solar corona	10^6	100	7.4	8.97×10^6	33.4	3.36×10^{11}	1.65×10^{-9}	
Solar atmosphere	10^{14}	1	7.4×10^{-5}	8.97×10^{10}	3.34×10^{-3}	3.36×10^3	3.55×10^{-4}	
Interstellar plasma	1.0	1	740	8.97×10^3	33.4×10^4	3.36×10^{17}	1.65×10^{-13}	
Strongly coupled plasma	10^{21}	0.2	1.05×10^{-8}	2.84×10^{14}	1.06×10^{-6}	3.36×10^{-4}	16.5	(*)
Shock tubes	10^{21}	0.2	7.40×10^{-6}	2.84×10^{12}	1.06×10^{-4}	3.36	0.036	

The electric charge disturbance $\delta\rho$ has spherical symmetry and equation (4.12) becomes,

$$\frac{d^2\phi}{dr^2} + \frac{2}{r}\frac{d\phi}{dr} - \frac{\phi}{\Lambda_D^2} = -\frac{q}{\varepsilon_o}\,\delta(r)$$

Because of the spherical symmetry only the radial distance $r > 0$ is considered and introducing $\phi\,(r) = a\,f(r)/r$ where $a > 0$ is constant,

$$\frac{a}{r}\left(\frac{d^2f}{dr^2} - \frac{1}{\Lambda_D^2}f\right) = -\frac{q}{\varepsilon_o}\,\delta(r)$$

For finite radial distances $r > 0$ where only ions and electrons are present and above equation reduces to,

$$\frac{d^2 f}{dr^2} - \frac{1}{\Lambda_D^2} f = 0$$

and possible solutions are,

$$f(r) = \exp(\pm\, r/\Lambda_D)$$

The function $\exp(r/\Lambda_D)$ is unphysical because the spatial perturbations in the plasma are amplified in this case. Furthermore, we need to recover the electric potential for a point charge placed at the origin $r = 0$ in the limit $r/\Lambda_D \ll 1$. The solution is then,

$$\phi_D(r) = \frac{a}{4\pi\varepsilon_o}\frac{e^{-r/\Lambda_D}}{r} \sim \frac{a}{r} \simeq \frac{q}{4\pi\varepsilon_o\, r}$$

gives the constant,

$$a = \frac{q}{4\pi\varepsilon_o}$$

and for the plasma bulk ($r > 0$) we have,

$$\phi_D(r) = \frac{q}{4\pi\varepsilon_o}\frac{e^{-r/\Lambda}}{r} \tag{4.14}$$

for the *Debye screening* of the electric charge disturbance. The perturbation in the plasma potential decays exponentially at a rate of $1 / \Lambda_D$ along the radial distance, as shown in figure 4.4. Equivalently, the external test charge perturbation $\delta\rho_{ex}$ is shielded by a cloud of opposite electric charge ρ_{sc} with a radius proportional to Λ_D .

Equation (4.13) relates the plasma density n_o and the temperatures T_i and T_e of charged particles to the shielding distance Λ_D, which accounts for the contribution to Debye shielding of electrons (λ_{De}) and ions (λ_{Di}). In LTE plasmas where ions and electrons are in thermal equilibrium $T_e \simeq T_i$ (high gas pressures in figure 4.1) the electron and ion Debye lengths are equal $\lambda_{De} \simeq \lambda_{Di}$. Having similar average kinetic energies, both charged species have comparable contributions to Debye shielding.

In contrast, ions are essentially cold, $T_e \gg T_i \simeq T_a$ and the electron Debye length is much longer $\lambda_{De} \gg \lambda_{Di}$ in PLE plasmas. The Debye shielding is essentially controlled by the higher average kinetic energy of lighter electrons. In low gas pressure plasmas, as in figure 4.1, the electron Debye length is mainly responsible for Debye shielding and is usually considered as the *plasma Debye length*.

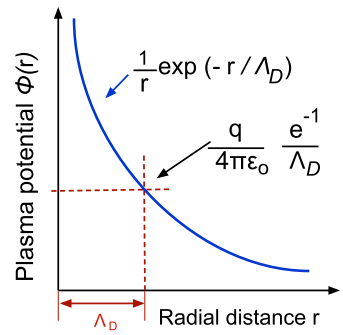

Figure 4.4. Exponential damping for the space fluctuations of the electric potential $\phi(r)$.

When no external test charge (or external electric field) is introduced in the plasma, only random fluctuations caused by the interaction between charged particles produce the deviation from quasineutrality. This effect is shown in the scheme of figure 4.3 where the local departure $\delta n_o(x)$ from plasma quasineutrality produces the thermal energy gained by charges to sustain the electric field fluctuation.

We mentioned before that the one-dimensional fluctuation of electric charge (figure 4.3) can be seen as two parallel sheets of electrons and ions separated a distance $d = \delta x$, similarly to a parallel square plates capacitor of side L. The total electric charge,

$$Q_c \simeq \pm e\ \delta n_o \times (\delta x \times L^2)$$

gives a surface charge density on each sheet,

$$\sigma_c = \pm \frac{e\ \delta n_o \times (\delta x) \times L^2}{L^2} = \pm e\ \delta n_o \times \delta x$$

and $E(x) \simeq E_o$ can be approximated by the electrostatic field in one dimension,

$$E_o \simeq \frac{\sigma_c}{\varepsilon_o} = \frac{e\ \delta n_o\ \delta x}{\varepsilon_o}$$

The electrostatic energy per particle is,

$$W_{el} = \int_o^{\delta x} e\ E_o\ dx = \frac{e^2\ \delta n_o (\delta x)^2}{\varepsilon_o}$$

which compares to the thermal energy per particle $W_{th} = \langle m v_x^2/2 \rangle = k_B\ T/2$ in one dimension. We can calculate the ratio,

$$\frac{W_{el}}{W_{th}} \sim \frac{e\phi}{k_B\ T} = \frac{e^2\ \delta n_o (\delta x)^2}{\varepsilon_o\ k_B T} = \left(\frac{\delta x}{\lambda_D}\right)^2 \ll 1$$

In ideal plasmas where $|e\ \phi/k_B T| \ll 1$ the random fluctuations δn_o from the plasma quasineutrality are extended along distances δx much shorter than the Debye length, as shown in the scheme of figure 4.3.

In table 4.1 the values of λ_D are calculated for the plasmas in figure 1.2 where the blue line at the lower side indicates the region where the Debye length is longer than 1 cm. Most space plasmas in this figure fall within this category and are *weakly coupled plasmas* where kinetic energy of particles is much higher than average potential energy of electric charges.

The ideal plasma *collectively responds* to perturbations produced by an external electric field or density fluctuations of plasma charged particles over longitudes much longer than the Debye length. Furthermore, we shall see in chapter 5 that Λ_D limits the effective distance for long-range Coulomb collisions between charged particles because Debye shielding attenuates the inter-particle electric fields.

It is important to emphasize that Debye shielding is realistic insofar as the magnitude of the perturbation introduced by the electric charge $\delta\rho_{ex}$ in equation

(4.9) is moderate. In *strongly coupled plasmas* where $\Gamma_c = (q\ \phi/k_B T_\alpha) > 1$ additional terms needs to be considered in the power expansion for $n_\alpha(\boldsymbol{r})$ in equation (4.11). The Poisson equation (4.12) transforms into a complex nonlinear differential equation and equation (4.14) for the plasma potential attenuation is no longer valid.

In the absence of Debye shielding, intense electric fields can develop in the plasma, as well as complex electrostatic structures as are the denominated *plasma double layers*. These are shown in figure 1.3 and are composed of different concentric plasma shells separated by abrupt changes in luminosity. These boundaries corresponds to plasma potential jumps (double layers) separating the different plasmas of the structure.

4.5.2 The plasma frequency

We will focus now on time dependent plasma fluctuations at a fixed point instead of the spatial propagation of disturbances from the equilibrium state. In figures 4.5 and 4.6 the spontaneous increase in the electron density is $n_e > n_i$ (similarly to the scheme of figure 4.3) over the circular region of area A, and diameter $\delta\, r$ locally breaks the plasma electrical neutrality. The excess of negative charge $\rho_c = e\ (n_i - n_e) < 0$ inside the cylindrical pillbox of figure 4.6 produces the radial E_r and axial E_z electric field components to restore the initial equilibrium.

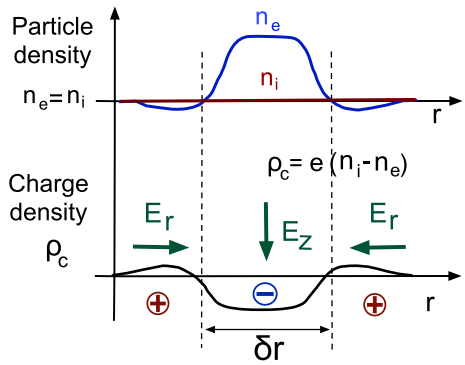

Figure 4.5. The fluctuation electron density n_e and electric charge ρ_c of figure 4.6 over δr.

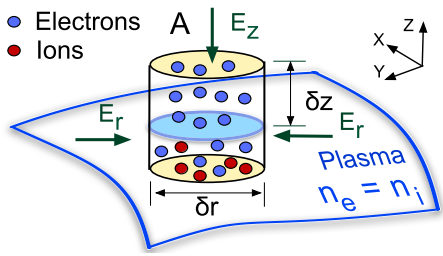

Figure 4.6. The negative charge fluctuation $\delta\ Q_e$ along δz creates the electric fields E_z and E_r.

The cylinder in figure 4.6 of cross sectional area A is divided into two parts by the surface (blue) that limits the quasineutral plasma placed below. The upper half of height δz contains the small excess of N_e electrons (blue dots), whereas the lower half (inside the plasma bulk) has electrons and ions (red dots).

The number of electrons within the upper half is $N_e = n_e\ A\ \delta z$ and the negative electric charge enclosed inside is $\delta\ Q_e = -\ e\ n_e\ A\ \delta z$. In the plasma surrounding the cylinder of figure 4.6 δQ_e produces the radial E_r and axial E_z components of the electric field. The latter pointing along the Z direction that can be calculated using equation (2.6a) and applying the Gauss' theorem to the pillbox,

$$\frac{\delta Q_e}{\varepsilon_o} = \int_{\text{box}} \boldsymbol{E} \cdot d\boldsymbol{s}$$

where $d\boldsymbol{s}$ is the external surface vector. Then,

$$\int_{\text{side}} \boldsymbol{E}_r \cdot d\boldsymbol{s} + \int_{\text{top}} \boldsymbol{E}_z \cdot d\boldsymbol{s} + \int_{\text{bott.}} \boldsymbol{E}_{\text{bottom}} \cdot d\boldsymbol{s} = -E_z\ A$$

and the contribution of the integral along the side faces is null because of the radial symmetry of the $\boldsymbol{E}_r$ component. The electric field $\boldsymbol{E}_{\text{bott}}$ over the bottom side of the pillbox intersecting the surface is also null because the plasma is quasineutral (equation (4.1); $n_e = n_i$ then $\boldsymbol{E}_{\text{bott}} \simeq 0$). We have $-A\ E_z = -e\ n_o A\ \delta z/\varepsilon_o$ and,

$$E_z = \frac{e}{\varepsilon_o}\ n_o\ \delta z$$

The mass of the electrons inside the upper half pillbox is $M_e = m_e N_e$ and its center of mass speed along the Z axis is $v_{cm} = d\delta z/dt$. The equation of motion for this electron group is,

$$M_e\ \frac{dv_{cm}}{dt} = -e\ \delta N_e\ E_z \quad \text{and we obtain,}$$

$$\frac{d^2}{dt^2}\delta z + \frac{e^2}{\varepsilon_o\ m_e}\ n_o\ \delta z = 0$$

If we multiply both sides of the last equation by $n_e\ A$ we derive the expression for the number of electrons $N_e = n_e A \delta z$ inside the top side of the pillbox in figure 4.6,

$$\frac{d^2 N_e}{dt^2} + \left(\frac{e^2\ n_e}{m_e\ \varepsilon_o}\right) N_e = 0$$

Therefore, the number of electrons N_e inside the upper half cylinder of figure 4.6 oscillates in time around the equilibrium state ($N_e = 0$, equivalent to $\delta z = 0$) driven by the electric field E_z with frequency,

$$\omega_{pe} = \sqrt{\frac{n_o\ e^2}{m_e\ \varepsilon_o}} \tag{4.15}$$

Box 4.3. Calculation of the electron plasma frequency

From equation (4.15) we have,

$$\omega_{pe}^2[\text{rad s}^{-1}] = \frac{e^2\, n_o}{\varepsilon_o\, m_e} = \frac{(1.6 \times 10^{-19})^2}{(8.85 \times 10^{-12}) \times (9.1 \times 10^{-31})} \times n_o\ [\text{m}^{-3}]$$
$$= 3179 \times n_o\ [\text{m}^{-3}]$$

and then

$$\omega_{pe}\ [\text{rad s}^{-1}] = 56.4 \times \sqrt{n_o\ [\text{m}^{-3}]}\ \text{equivalently,}$$
$$\omega_{pe}[\text{rad s}^{-1}] = 56\,400 \times \sqrt{n_o\ [\text{cm}^{-3}]}$$

Finally, $f_{pe} = \omega_{pe}/2\pi$ and we obtain,

$$f_{pe}\ [\text{Hz}] = 8.97 \times \sqrt{n_o\ [\text{m}^{-3}]}\ \text{or,}$$
$$f_{pe}\ [\text{Hz}] = 8970 \times \sqrt{n_o\ [\text{cm}^{-3}]}$$

The ion plasma frequency depends on its mass m_i and values of the electron plasma frequency for different plasmas are calculated in table 4.1.

This last expression defines the *electron plasma frequency* $f_{pe} = \omega_{pe}/2\pi$ also called *Langmuir frequency* and a practical formula to calculate f_{pe} is derived in box 4.3. Similar arguments as above apply to ions and the *ion plasma frequency* f_{pi} is also introduced for positive charges. The ratio,

$$f_{pi} = f_{pe}\sqrt{\frac{m_e}{m_i}} \ll f_{pe}$$

shows *the shortest plasma time scale* that is related to electron oscillations. It should be remarked that ion and electron plasma frequencies only rely on the equilibrium charged particle density $n_i = n_e$ and are independent of the temperatures of charged particle species.

We can also see the temporal scale $\tau_{pe} = 1/f_{pe}$ associated with the electron plasma frequency as proportional to the time a thermal electron with speed $v_{th} = \sqrt{2k_B T_e/m_e}$ travels along one Debye length.

$$\frac{\lambda_D}{V_{Te}} = \left(\frac{\varepsilon_o m_e}{2\, n_e\, e^2}\right)^{1/2} = \frac{1}{\sqrt{2}\ \omega_{pe}} = \frac{1}{2\pi\ \sqrt{2}\ f_{pe}} \sim \tau_{pe}$$

The frequency $f_{pe} = 1/\tau_{pe}$ determines the fastest response time τ_{pe} for lighter particles (electrons) to time dependent fluctuations. This temporal scale is much shorter than

that corresponding for ions $\tau_{pi} \gg \tau_{pe}$ which is determined by the ion plasma frequency.

When the charge density of a quasineutral plasma is perturbed with low frequencies $f = 1/\tau \ll (f_{pe}, f_{pi})$, or equivalently, on a temporal scale $\tau \gg (\tau_{pe}, \tau_{pi})$ much longer than ion and electron response times, both electrons and ions can move rapidly. The attenuation of fluctuations by charged plasma particles is much faster than the time scale of the disturbance, which produces the essentially stationary Debye shielding effects discussed in the previous section 4.5.1.

The longer ion response time $\tau_{pi} \ll \tau_{pe}$ becomes important when the characteristic frequency of fluctuations is further increased to $f_{pi} < f \ll f_{pe}$ and for these intermediate frequencies where $\tau_{pi} < \tau \ll \tau_{pe}$ the electrons still have a fast response but the motion of ions can be regarded as *frozen* on this temporal scale. In this intermediate frequency range the ions respond to perturbations via *ion acoustic waves* that are analogous to sound waves in neutral fluids. Finally, for high frequencies $f_{pi} < f_{pe} < f$ the motion of both electrons and ions is hindered and the system responds collectively, oscillating at the plasma frequency.

The values of $f_{pe} = \omega_{pe}/(2\pi)$ are calculated in table 4.1 for plasmas of figure 1.2, the corresponding values for f_{pi} are much lower and depend on the mass of ions. For argon gas with mass number $A = 40$ we have,

$$f_{pi} = f_{pe} \times \left(\frac{1}{1840 \times 40}\right)^{1/2} = f_{pe} \times \frac{1}{271}$$

and in table 4.1 we have $f_{pe} = 8.97$ GHz and $f_{pi} = 33.1$ MHz. In figure 1.7 the electron plasma densities are between $n_e \sim 1\text{–}5 \times 10^5$ cm^3 in daylight for altitudes between 100–500 km and this gives $f_{pe} \sim 2.84\text{–}6.34$ MHz, whereas f_{pi} depends on the variable chemical composition of the ionosphere.

Denser fusion and strongly coupled laser plasmas have much higher values for f_{pe} in the range $f_{pe} \sim 284\text{–}8970$ GHz, whereas low pressure PLE and glow discharges have 8.97 GHz and $f_{pe} \sim 89.7$ kHz in table 4.1.

4.5.3 The plasma and coupling parameters

The *weakly coupled* or *ideal plasma* $\Gamma_c < 1$ approximation in equations (4.8) and (4.10) requires a minimum number of charges to shield the external disturbances. Otherwise, Debye shielding would not be a statistically valid concept. In the quasineutral plasma of density n_o,

$$N_{De} = n_o \times \lambda_{De}^3$$

is the number of electrons inside a cube with side λ_{De} and defines the dimensionless *plasma parameter* for electrons and the equivalent expression N_{Di} for ions.

The Debye lengths of ions and electrons are equal and $N_{De} = N_{Di}$ in LTE plasmas, whereas $N_{De} \gg N_{Di}$ in PLE where $T_e \gg T_i$ and Debye shielding is essentially due to electrons.

The plasma parameter $N_{D\alpha}$ is also related with the dimensionless *coupling parameter* $\Gamma_{c\alpha} = e\phi/k_B T_\alpha$ introduced in equation (4.8) as the ratio between the

electrostatic and thermal energies. Alternatively, $\Gamma_{c\alpha}$ could also be defined as the quotient between the minimum approach distance r_c between repelling charges (see figure 4.7) and the average length[9] $d_o = n_o^{-1/3}$ between plasma particles.

The potential energy of two repelling charged particles is,

$$E(r,\, v_\alpha) = \frac{1}{2} m_\alpha\, v_\alpha^2 - \frac{e^2}{4\pi\varepsilon_o\, r}$$

The minimum distance of approach r_c is when $E\ (r_c,\ v_\alpha) = 0$ and gives $r_c = e^2/(4\pi\ \varepsilon_o\ v_\alpha^2)$. Substituting the thermal speed $v_{th,\,\alpha} = (2k_B T_\alpha/m_\alpha)^{1/2}$ we have on average,

$$\langle r_c \rangle = \frac{e^2}{4\pi\varepsilon_o k_B T_\alpha}$$

Then $\langle r_c \rangle$ is also the average distance where the potential energy of colliding particles equals their kinetic energy and,

$$\Gamma_{c\alpha} = \frac{\langle r_c \rangle}{d_o} = \frac{e^2\ n_o^{1/3}}{4\pi\ \varepsilon_o\ k_B T_\alpha} \tag{4.16}$$

This new definition of the coupling parameter is equivalent to equation (4.8),

$$\Gamma_{c\alpha} = \frac{\langle r_c \rangle}{d_o} = \frac{e^2}{4\pi\ \varepsilon_o\ r_d\ k_B T_\alpha} = \frac{e^2}{4\pi\ \varepsilon_o\ d_o} \times \frac{1}{k_B T_\alpha}$$

and then,

$$\Gamma_{c\alpha} = \frac{e\ \phi(d_o)}{k_B T_\alpha} \sim \frac{\langle E_{el} \rangle}{\langle E_{th} \rangle}$$

where $\langle E_{th} \rangle \sim \phi(d_o) = e/(4\ \pi\ \varepsilon_o\ d_o)$ is the average electric potential created by neighboring plasma particles.

The coupling $\Gamma_{c\alpha}$ and plasma $N_{D\alpha}$ parameters are related,

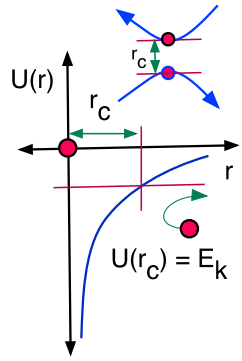

Figure 4.7. The minimum distance r_c between two repelling charges.

[9] The distance d_o is also denominated Wigner–Seitz radius.

$$\Gamma_{c\alpha} = \frac{e^2\, n_o^{1/3}}{4\pi\, \varepsilon_o\, k_B T_\alpha} = \frac{1}{4\,\pi} \times \frac{e^2\, n_o}{\varepsilon_o\, k_B T_\alpha} \times \frac{n_o^{1/3}}{n_o}$$
$$= \frac{1}{4\,\pi} \times \lambda_{D\alpha}^{-2} \times n_o^{-2/3} = \frac{1}{4\,\pi} \times \frac{1}{\left[n_o\, \lambda_{D\alpha}^3\right]^{2/3}}$$

where $N_{D\alpha} = n_o\, \lambda_{D\alpha}^3$ and,

$$\Gamma_{c\alpha} \sim \frac{1}{4\,\pi} \frac{1}{\left(n_o\, \lambda_{D\alpha}^3\right)^{2/3}} \sim \frac{1}{4\,\pi} \frac{1}{N_{D\alpha}^{2/3}} \tag{4.17}$$

The coupling parameter $\Gamma_c \gg 1$ is large in *strongly coupled plasmas* where $N_D \ll 1$ and the Debye cube contains few charged particles. In the opposite case of a *weakly coupled* $\Gamma_c \ll 1$ we have $N_D \gg 1$ and a large number of particles are within the cube of volume λ_D^3.

In table 4.1 are calculated the Γ_c and N_D for plasma of figure 1.2 where the green upper line in the scheme of figure 1.2 indicates the region ($N_D \sim n_o \lambda_D^3 \ll 1$) where the Debye sphere is scarcely populated. The dense and cold *strongly coupled plasmas* are indicated by an asterisk in table 4.1 and—strictly speaking—the Debye length is not a statistically valid concept in this case[10]. In contrast, *ideal Maxwellian plasmas* are weakly coupled and a large number of charged particles are involved in the collective response to external disturbances over characteristic longitudes longer than the Debye length.

4.5.4 Magnetized plasmas

After studying the plasma under an external electric field we will characterize its response to the magnetic field. In both cases free charges will oppose the external disturbance, so that the plasma will essentially have a *diamagnetic response*[11]. In *magnetized plasmas* the strength of local magnetic field is high enough to alter the trajectories of charged particles, which are accelerated by the Lorentz force (2.5)

$$\boldsymbol{F}_\alpha = q_\alpha\, (\boldsymbol{E} + \boldsymbol{v}_q \times \boldsymbol{B})$$

in the frame of reference where the magnetic field lines of the magnetic flux density $\boldsymbol{B}$ remain at rest. The force experienced by the charges is null along the direction parallel to $\boldsymbol{B}$, whereas they move circular orbits in the perpendicular plane with a *cyclotron frequency* or *gyrofrequency*,

$$\Omega_\alpha = \frac{B\, q_\alpha}{m_\alpha}$$

[10] The power expansion of equation (4.11) to approximate $n_e(\boldsymbol{r})$ and $n_i(\boldsymbol{r})$ is only valid when $(e\phi/k_B T) \ll 1$.
[11] The strength of the magnetic field decreases in the plasma bulk by the opposite effect produced by the response of charged particles, contrary to *paramagnetic* media.

The *Larmor radius* or *gyroradius* of a charged particle α is the ratio between the component of the velocity $\boldsymbol{v}_\perp$ perpendicular to the magnetic file lines and the gyrofrequency Ω_α,

$$R_{l\alpha} = \frac{v_\perp}{\Omega_\alpha}$$

This magnitude is estimated using l_α where $v_\perp$ the particle thermal speed $v_{th,\ \alpha}$ is employed in place of $v_\perp$ and then,

$$l_\alpha = \frac{v_{th,\ \alpha}}{\Omega_\alpha} \text{ and therefore, } l_e = \sqrt{\frac{m_e}{m_i}}\ l_i$$

The plasma is said to be *magnetized* when l_α is comparable with the relevant length scale L_s and *unmagnetized* otherwise. In accordance with the magnitude of $\boldsymbol{B}$ we found situations where $l_e / L_s \sim 1$ while $l_i / L_s \ll 1$ so that *electrons can be magnetized*, whereas the ions are not. However, when we refer to a *magnetized plasma* we usually mean that both species, ions and electrons are magnetized.

4.5.5 Magnetic shielding

Under the influence of an external magnetic field, the motion of charged particles produces currents which create in turn magnetic fields opposed to the external perturbation. The force that moves the charges is the electromotive induction force due to the temporal variations of the magnetic field. The scheme of figure 4.8 represents the effects of the magnetic field located at $x \leqslant 0$ in the ideal plasma of density n_o placed in the half-plane $x > 0$ in steady state. The one-dimensional magnetic flux density is given by,

$$\boldsymbol{B}(x,\ t) = \begin{cases} B_o(t)\ \boldsymbol{k} & \text{if } x = 0 \\ B_z(x,\ t)\ \boldsymbol{k} & \text{if } x > 0 \end{cases} \tag{4.18}$$

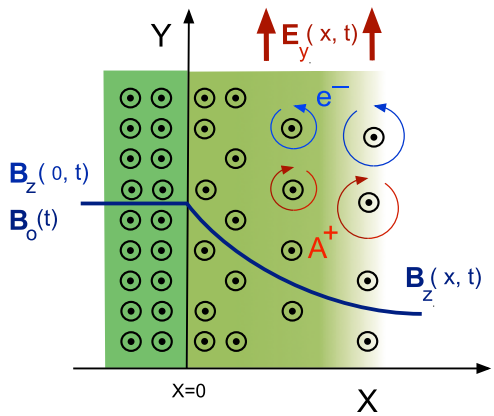

Figure 4.8. The external magnetic field placed at $x < 0$ penetrates in the plasma located in the half plane $x \geqslant 0$.

The plasma electrons (e^- are blue arrows) and ions (A^+ are red arrows) perform circular motions in opposite directions on perpendicular planes to the magnetic field lines. Because of the symmetry, no transport of charged particles exists along the Z axis, that points to the reader.

In this situation equation (2.6b) of the Maxwell equations (2.6) for $x > 0$ is,

$$\frac{\partial \boldsymbol{B}}{\partial t} = \frac{\partial B_z}{\partial t} k = -\nabla \times \boldsymbol{E} = -(\frac{\partial E_y}{\partial x} - \cancelto{0}{\frac{\partial E_x}{\partial y}}) k$$

For symmetry the electric field component $E_y(x, t)$ takes the same constant value along of Y axis. Equation (2.6d) gives,

$$\nabla \times \boldsymbol{B} = -\frac{\partial B_z}{\partial x} \boldsymbol{j} = \mu_o \boldsymbol{J}_c + \mu_o \varepsilon_o \frac{\partial \boldsymbol{E}}{\partial t}$$

The electric current density of plasma particles $\boldsymbol{J}_c = \boldsymbol{J}_{xc} + \boldsymbol{J}_{yc}$ has two components as well as the electric field $\boldsymbol{E} = E_x(x, t)\, \boldsymbol{i} + E_y(x, t)\, \boldsymbol{j}$. We obtain,

$$-\frac{\partial B_z}{\partial x} = \mu_o J_{yc} + \frac{1}{c^2} \frac{\partial E_y}{\partial t} \text{ and, } 0 = \mu_o J_{xc} + \frac{1}{c^2} \frac{\partial E_x}{\partial t}$$

We consider a time scale $\omega_{pi}^{-1} > \tau_c \gtrsim \omega_{pe}^{-1}$ so that, the time derivatives of the fields $B_z(x, t)$, $E_y(x, t)$ and $E_z(x, t)$ are very small compared to c^2 and we can thus neglect the second terms in the above equations. Additionally, the motion of ions remains essentially *frozen* and the electric current mainly due to the faster electrons,

$$-\frac{\partial B_z}{\partial x} \simeq \mu_o J_{c,\,y} = -\mu_o\, e\, n_o\, u_e$$

where u_e is the electron speed. In these conditions the electron current along the X axis $J_{xc} \simeq 0$ can be also neglected and along the Y axis the equation of motion for electrons is,

$$\frac{\partial u_e}{\partial t} = -\frac{e}{m_e} E_y(x, t)$$

the fields are related by,

$$\frac{\partial B_z}{\partial t} = -\frac{\partial E_y}{\partial x} \text{ and, } \frac{\partial B_z}{\partial x} = \mu_o\, e n_o\, u_e$$

Eliminating u_e and B_z and setting $E_y(x, t) = S(x)\, G(t)$ we obtain a differential equation for $S(x)$ as,

$$\frac{\partial^2 S}{\partial x^2} = \frac{e^2\, \mu_o\, n_o}{m_e} S(x) = \frac{\omega_{pe}^2}{c^2} S(x)$$

and we have,

$$E_y(x, t) = E_o\, G(t) e^{-x\, (\omega_{pe}/c)}$$

The time dependence $G(t)$ can be determined using equation (4.18) in $x = 0$ and $\partial B_z/\partial t = \partial E_y/\partial x$ and finally,

$$\boldsymbol{E}_y(x, t) = \lambda_L \left(\frac{\partial B_o}{\partial t}\right) e^{-x/\lambda_L} \boldsymbol{j} \tag{4.19}$$

and also,

$$\boldsymbol{B}_z(x, t) = B_o(t) e^{-x/\lambda_L} \boldsymbol{k} \tag{4.20}$$

The induced electric field (4.19) and the magnetic flux density (4.20) in the plasma located at $x > 0$ of figure 4.8 exponentially decrease along the x coordinate at a rate $\lambda_L = c / \omega_{pe} > 1$ denominated *collisionless skin depth* or *London length*.

The spatial attenuation of equations (4.19) and (4.20) in figure 4.8 illustrates the plasma *diamagnetic response* to external magnetic fields. The *external* magnetic field is attenuated by the circular motion of charged particles (essentially electrons) that produce local magnetic fields opposed to the perturbation.

Specifically, alternating electromagnetic fields are damped inside conductive media (plasma, metals, etc) by electric currents flowing only near their surfaces. This is called *skin effect* and is characterized in ideal plasmas by the collisionless London length $\lambda_L = c/\omega_{pe} \sim 1/\sqrt{n_o}$ decreasing with the plasma density n_o.

In consequence, the propagation of electromagnetic waves in the plasma region is limited (as in metals) by the distance λ_L that governs the depth of penetration of $\boldsymbol{B}(x, t)$ into the plasma media. Table 4.1 shows the values of λ_L for plasmas in figure 1.2 which are calculated in meters. The London lengths are usually much longer than typical longitudes involved in the experiments for low density laboratory plasmas, but are much shorter than those involved in planetary and solar space environments. Therefore, time dependent external magnetic fields penetrate in the system and can influence the motion of charged particles. In the opposite limit of denser fusion and laser produced plasmas, λ_L can fall below the characteristic size of experiments.

In all cases, the plasma frequency governs the electron response and frequencies $\omega \gg \omega_{pe}$ of the electromagnetic field pass straight through the plasma because electrons and ions cannot follow the time dependent perturbation. The energy of the external electromagnetic field is not lost by moving electrical charges and/or inducing electromagnetic fields in the plasma. On the contrary, for frequencies part of the energy is spent inducing electric currents in the skin depth, as in figure 4.8. The electromagnetic fields are attenuated in the plasma and the wave is reflected, in the same way as by the surface of a metal.

The electron densities in the ionosphere, between 10^5–10^6 cm^{-3} depend on the altitude and the local plasma frequencies change accordingly. The very high frequency (VHF) radio signals, typically over 30 MHz, are well over ω_{pe} of the ionospheric plasmas and pass straight through. Lower signal frequencies can be reflected back towards the Earth's surface by the different plasma layers in the ionosphere.

4.6 Commentaries and further reading

The concept of *ideal* plasma is introduced in sections 6.1.1 and 11.8.3 of reference [1] and in reference [3], where also *dusty plasmas*[12] are discussed as example of *non-ideal* plasma. Furthermore, section 3.1 of reference [4] has a short discussion of *ideal plasmas* in the present context. References [1, 5] and [6] discuss in detail the kinetics of charged particles connecting the elementary processes with plasma chemistry.

The general formulation of the *principle of detailed balancing* is complex but in chapter 7, section 1.1 of reference [7] can be found a short discussion on this subject. The cross section for each reaction and its inverse process are related by the principle of microscopic reversibility and detailed balancing can be used to obtain information about the counterpart collision, and reference [6] discusses a practical application in section 8.5 of chapter 8.

The characteristics and properties of thermodynamic (CTE) and kinetic plasma equilibrium states (LTE and PTE) in connection with this principle are addressed in section 4.1.6 of reference [1]. A recent thorough discussion of the plasma equilibrium states can be found in chapter 1 of the book [8]. The *skin effect* is introduced in section 3.3 of the book [9], including collisions with neutrals in section 12.1 of [6] and also discussed in detail in the comprehensive paper [10].

References

[1] Fridman A and Kennedy L A 2004 *Plasma Physics and Engineering* (New York: Taylor and Francis)
[2] Roth J R 1995 *Industrial Plasma Engineering* vol 1 (Bristol: Institute of Physics Publishing)
[3] Fortov V R and Iakubov I T 2000 *The Physics of Non-ideal Plasma* (Singapore: Word Scientific)
[4] Smirnov B M 2001 *Physics of Ionized Gases* (Chichester: Wiley)
[5] Raizer Y P 1991 *Gas Discharge Physics* (Berlin: Springer)
[6] Lieberman M A and Lichtenberg A J 1994 *Principles of Plasma Discharges and Materials Processing* (New York: Wiley)
[7] Bittencourt J A 2004 *Fundamentals of Plasma Physics* 3rd edn (New York: Springer)
[8] Nguyen-Kuok S 2017 *Theory of Low-temperature Plasma Physics* (Cham: Springer)
[9] Rax J-M 2007 *Physique des Plasmas* (Paris: Dundod)
[10] Kobolov V and Economou D 1997 The anomalous skin effect in gas discharge plasmas *Plasma Sources Sci. Technol.* **6** R1–17

[12] Plasmas with charged solid particles in addition to ions and electrons.